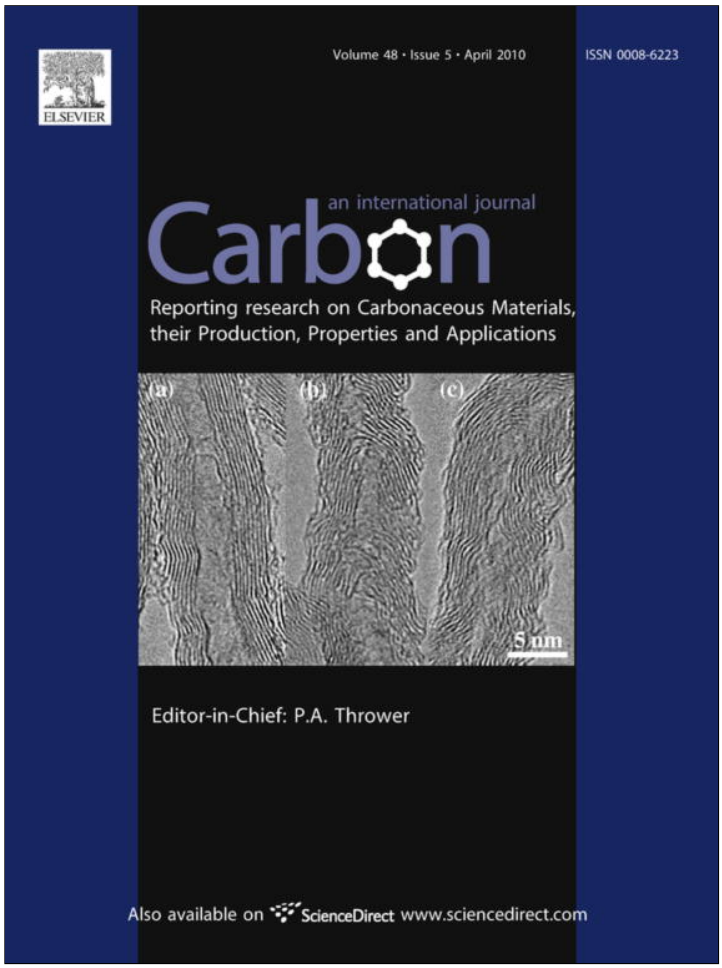

CARBON 48 (2010) 1457–1464

available at www.sciencedirect.com

ScienceDirect

journal homepage: www.elsevier.com/locate/carbon

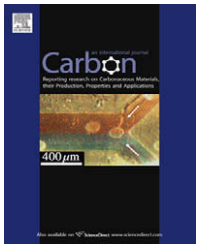

Unprecedented vibration damping with high values of loss modulus and loss tangent, exhibited by cement–matrix graphite network composite

Sivaraja Muthusamy [1], *Shoukai Wang*, *D.D.L. Chung* *

Composite Materials Research Laboratory, University at Buffalo, State University of New York, Buffalo, NY 14260-4400, USA

ARTICLE INFO

Article history:
Received 21 November 2009
Accepted 17 December 2009
Available online 23 December 2009

ABSTRACT

This paper reports a material with unprecedented vibration damping ability, as shown by high values of both the loss tangent (vibration amplitude decay rate) and the loss modulus (energy dissipation ability, equal to the product of the storage modulus and the loss tangent) under flexure at 0.2 Hz at room temperature. The loss modulus (7.5 GPa) exceeds that of any previously reported material, including the best metal-based material, which suffers from a low loss tangent. The loss tangent (0.81) is comparable to or exceeds that of any previously reported material, including rubber, which suffers from a low loss modulus. This material is a cement–matrix graphite network composite containing 8 vol.% graphite and made by compressing a mixture of cement particles and exfoliated graphite, which binds by mechanical interlocking, followed by curing in water. The graphite network structure is supported by microscopy and the low electrical resistivity of the composite (0.04 Ω cm perpendicular to the compression direction and 0.5 Ω cm in the compression direction). The composite is much more conductive than the most conductive cement–matrix composite containing a conductive admixture. The high loss tangent is attributed to the graphite network, while the high storage modulus is attributed to the cement matrix.

1. Introduction

Vibration damping refers to the reduction of mechanical vibrations, which can adversely affect a structure. Structures such as bridges, buildings, nuclear reactors, robots, rotating machinery, micromachines, optics and microelectronics benefit from vibration damping, which enhances safety, user comfort, performance, reliability, durability, seismic resistance and blast resistance.

Vibration damping is related to sound attenuation, since a sound wave is a form of vibrational wave. Therefore, materials that are effective for vibration damping tend to be effective for sound attenuation as well.

Vibration damping can be achieved passively or actively. Active damping involves the use of a coordinated set of sensor and actuator, so that the actuator suppresses the vibration through force application in real time as the vibration sensed by the sensor occurs. Due to the sensor and actuator, active damping is expensive. However, it is highly effective. A much less expensive and much more common method of damping is passive. In passive damping, materials that are inherently effective for damping are utilized for dissipating the energy associated with the vibration; sensors and actuators are not used. This paper relates to passive damping.

The damping ability of a material is described by (i) the loss tangent (two times the damping ratio), which describes

* *Corresponding author:* Fax: +1 716 645 2883.
E-mail address: ddlchung@buffalo.edu (D.D.L. Chung).
URL: http://alum.mit.edu/www/ddlchung (D.D.L. Chung).
[1] Current address: Department of Civil Engineering, Kongu Engineering College, Perundurai, Erode 638 052, India.
0008-6223/$ - see front matter
doi:10.1016/j.carbon.2009.12.040

the ability for decay of the vibration amplitude and (ii) the loss modulus (the storage modulus times the loss tangent), which describes the energy dissipation ability. Both attributes should be high for effective damping.

Previously reported damping materials fall into three categories: (i) materials exhibiting high loss modulus but low loss tangent (such as cast iron, metal–matrix composites [1–3], shape-memory alloys [4–7] and acrylic impregnated ceramics [8]), (ii) materials exhibiting high loss tangent but low loss modulus (such as rubber and other polymers [9,10]), and (iii) materials exhibiting low values of both loss tangent and loss modulus (such as quartz particle filled epoxy [11], short carbon fiber filled nylon [12], interpenetrating polymer networks [13], hot-compacted polyethylene/polypropylene [14] and short jute fiber filled polymer blend [15]). Tables 1 and 2 provide a summary of the damping properties of previously reported materials. This paper reports a material with unprecedented vibration damping ability, with high values of both loss modulus and loss tangent.

Cement-based materials are important for the civil infrastructure. The damping ability of cement paste has been improved substantially by the use of admixtures, such as silica fume, latex and methylcellulose [16–18], but the values of both loss tangent and loss modulus remain low (Table 1). By using as admixtures silica fume (silica particles of mean size 0.1–0.2 μm) in the amount of 15% by mass of cement, together with methylcellulose in the amount of 0.4% by mass of cement, both the loss modulus and the loss tangent have been increased [16] (Table 1). By using silica fume in the absence of methylcellulose, the damping improvement is less [18]. By using silane-treated silica fume, the damping improvement has been further improved slightly [17]. By using either latex (styrene–butadiene copolymer) particles or methylcellulose (dissolved in water) in the absence of silica fume as an admixture, the damping behavior is inferior to that attained by using silica fume [18] (Table 1). In particular, the use of latex causes the loss tangent to increase by a greater extent than the use of silica fume, but the storage modulus is increased by a lesser extent, so that the overall damping ability is inferior [16,18] (Table 1). The effects of carbon fiber [16] or carbon nanotube [19] on the damping behavior are small compared to those of silica fume, latex or methylcellulose. The effect of polyethylene fiber [16] is even less than that of carbon fiber.

In contrast to the low loss tangent of these cement-based materials is the high value of rubber (Table 1) [20], which, however, suffers from a low loss modulus. On the other hand, metal–matrix composites have high values of the loss modulus (Table 1) [21], but they suffer from low values of the loss tangent. No material of the prior art has high values of both loss modulus and loss tangent at the same temperature.

In general, the loss tangent, elastic modulus and loss modulus are properties that vary with temperature for a given material. For example, for a thermoplastic polymer, softening upon heating increases the loss tangent but decreases the elastic modulus. Thus, the loss tangent is relatively high, but the elastic modulus is relatively low after softening; whereas the loss modulus is relatively high, but the loss tangent is relatively low before softening. In contrast, this paper provides a material that exhibits high values of both loss modulus and loss tangent at the same temperature, namely room temperature, which is the temperature that is most relevant to applications.

The material of this paper is a cement–matrix composite containing a graphite network (8 vol.%) formed by compressing exfoliated graphite. The shear deformation ability (somewhat like rubber) of the graphite network enables the loss tangent to be high, while the stiff cement matrix provides a high storage modulus. The combination of a high loss tangent and a high storage modulus results in a high loss modulus. Under flexure at 0.2 Hz, the loss modulus of the composite

Table 1 – Dynamic flexural properties obtained under three-point bending at 0.2 Hz and room temperature. The cement/graphite composites (first three entries) pertain to this work. The other materials are prior work in the authors' laboratory. All data in this table were obtained using the same testing method.

Cement/graphite volume ratio	Graphite volume fraction[a]	Storage modulus (GPa)	Loss tangent	Loss modulus (GPa)	Figure of merit ($GPa^{1/2}$)[b]
7:1 (this work)	0.13	2.70 ± 0.12	0.425 ± 0.034	1.148 ± 0.056	0.70
9:1 (this work)	0.10	6.84 ± 0.20	0.634 ± 0.022	4.337 ± 0.110	1.66
12:1 (this work)	0.077	9.26 ± 0.16	0.811 ± 0.045	7.502 ± 0.224	2.47
Neoprene rubber [20]		0.00745	0.67	0.0067	0.058
PMMA [20]		3.63	0.093	0.336	0.18
Flexible graphite [28]		1.0	0.19	0.21	0.19
Cement paste (plain) [16,18]		1.91	0.035	0.067	0.048
Cement paste with methylcellulose (0.4%[c]) [16,18]		4.12	0.073	0.301	0.15
Cement paste with methylcellulose (0.8%[c]) [18]		4.53	0.104	0.471	0.22
Cement paste with latex (20%[c]) [16,18]		2.75	0.122	0.336	0.20
Cement paste with latex (30%[c]) [18]		3.12	0.142	0.443	0.25
Cement paste with silica fume (15%[c]) [18]		5.76	0.107	0.616	0.26
Cement paste with silica fume (15%[c]) and methylcellulose (0.4%[c]) [16,17]		6.20	0.105	0.651	0.26
Zn–Al matrix SiC whisker composite [21]		99	0.032	3.0	0.32

[a] Before curing. The value is slightly lower after curing.
[b] Defined as the product of the loss tangent and the square root of the elastic modulus.
[c] % per mass of cement.

Table 2 – Dynamic flexural properties obtained by various prior workers using various testing methods at the optimum reported temperature for each material.

Material	Storage modulus (GPa)	Loss tangent	Loss modulus (GPa)	Figure of merit ($GPa^{1/2}$)[a]
Nanoscale Cu–Al–Ni shape-memory alloy [4]	22.6	0.196	4.43	0.93
Tungsten (95%) with In–Sn [4]	161	0.05	8.1	0.63
Acrylic impregnated ceramic [8]	60	0.04	2.4	0.31
Quartz particle filled epoxy [11]	3	0.15	0.45	0.26
Short carbon fiber filled nylon [12]	13	0.05	0.7	0.2
Interpenetrating polymer networks [13]	0.13	0.3	0.040	0.11
Hot-compacted polyethylene/polypropylene [14]	5.4	0.083	0.45	0.19
Short jute fiber filled polymer blend [15]	1	0.1	1	0.1

[a] Defined as the product of the loss tangent and the square root of the elastic modulus.

(7.5 GPa) (Table 1) exceeds that of metal–matrix composites (e.g., 3.0 GPa [21], Table 1), which suffer from a low loss tangent (e.g., 0.03 [21], Table 1), while the loss tangent of the composite (0.81, Table 1) exceeds that of rubber (0.67 [20], Table 1), which suffers from a low loss modulus (6.7 MPa [20], Table 1). All materials in Table 1 are tested using the same set-up (Section 2) for reliable comparison.

Ref. [4] compares the damping behavior of a large number of polymers, metal alloys, intermetallic compounds, shape-memory alloys, metal–matrix composites and ceramics and reports the best performance (loss tangent 0.196, elastic modulus 22.6 GPa, and loss modulus 4.43 GPa) for a nanoscale Cu–Al–Ni shape-memory alloy (Table 2). The loss tangent and loss modulus of the best composite of this work (Table 1) are higher than those of the best material of Ref. [4].

Ref. [4] uses a figure of merit defined as the product of the loss tangent and the square root of the elastic modulus. Among previously reported damping materials, the highest value of the figure of merit is 0.93 $GPa^{1/2}$, as shown by the best material (a nanoscale shape-memory alloy) of Ref. [4], but this material suffers from a low value of the loss tangent (Table 2). In terms of the figure of merit, the second highest performance damping materials of the prior art is tungsten with In–Sn [4], but this material suffers from a low value of the loss tangent (Table 2). In contrast, the best composite of this work exhibits a figure of merit, namely 2.47 $GPa^{1/2}$, that is above those of the best previously reported materials (Table 1).

The composites of this work are made from exfoliated graphite and cement particles. In contrast, prior work on cement–graphite composites involve either graphite flakes (not exfoliated) or carbon fibers (not exfoliated) for tailoring the thermoelectric behavior [22,23], electromagnetic shielding behavior [24] or the electrochemical behavior [25].

Exfoliated graphite is obtained by intercalating graphite flake and then exfoliating the flake by rapid heating [26]. The exfoliation results in an accordion microstructure. It is known that, upon compression of exfoliated graphite without a binder, a structure known as flexible graphite [27,28] is formed, due to the mechanical interlocking enabled by the accordion microstructure. Flexible graphite is moderately attractive for damping. Its loss tangent is much lower than that of rubber, though its figure of merit is higher than that of rubber (Table 1) [28].

The objectives of this work are (i) to provide a material with high values of both loss tangent and loss modulus, thereby providing a material with unprecedentedly high vibration damping ability, (ii) to provide a method of making the material mentioned in (i), (iii) to characterize the material mentioned in (i) in terms of the static mechanical properties (modulus and strength under flexure and compression), which are relevant to structural applications, and (iv) to characterize the material mentioned in (i) in terms of the electrical resistivity, as a low resistivity is attractive for electrical grounding, lightning protection, electrostatic discharge protection, electromagnetic shielding (which is needed for the protection of electronics from radio frequency radiation) electromagnetic pulse protection and deicing (by resistance heating).

2. Experimental methods

The exfoliated graphite is obtained by rapid furnace heating of acid intercalated graphite, which is known as expandable graphite (made from natural graphite flakes), as provided as GrafGuard (Grade 160–80 N) by GrafTech International, Lakewood, OH. Heating of the expandable graphite above 160 °C causes gas evolution and hence exfoliation, according to the manufacturer. The flakes are of typical mean size 0.25 mm (65% on 80 mesh), with specific volume 1.25 cm^2/g. Exfoliation at 600 °C gives a specific volume of 200 cm^3/g, according to the manufacturer. In this work, the heating is conducted in a stainless steel foil tubing of length 65 cm, with flowing nitrogen, by using a Lindberg tube furnace at 1000 °C, with the expandable graphite flakes exposed to this temperature for 2 min. After exfoliation, the worms (a worm referring to the exfoliated graphite obtained from a single graphite flake) are of length 2–4 mm.

Cement is Type I Portland Cement, as provided by Quikrete International Inc., Atlanta. The particle size of the cement is reduced by ball milling, using ceramic cylinders as the grinding medium which, along with the cement particles, is contained in a ceramic container during the milling. The ball milling time is 12 h. The milling reduces the particle size of the cement from a maximum of 90 μm to a maximum of 75 μm. Without the size reduction, the composites are much inferior. No aggregate is used.

The exfoliated graphite is mixed with cement particles prior to compression to form a sheet. After this, the sheet is exposed to water for the purpose of curing the cement in the sheet. The water exposure involves exposure to moisture

for 2 days, followed by immersion in water for 26 days. After 7 days of water immersion (when the sheet is not yet very hard), the sheet is temporarily removed from the water and cut into specimens of sizes that are appropriate for various tests. After the cutting, the specimens are immediately immersed in water for further curing. Curing in moisture without water immersion gives inferior composites.

The weights of the exfoliated graphite and cement in the mixture are controlled. The mixing is conducted in the dry state at room temperature for 24 h using a ball mill without any grinding medium. The compression of the mixture is conducted in the dry state in a cylindrical mold of length 45 cm and inner diameter 31.75 mm by applying a uniaxial pressure of 5.6 MPa (1000 lb) via a matching piston. The entire thickness of a composite specimen is obtained in one 5.6 MPa compression stroke. Each resulting specimen is a disc of diameter 31.75 mm and thickness ranging from 1.5 to 2.0 mm. The thickness varies among the discs and is separately measured for each disc.

Each disc is cut by using a knife into a number of specimens (Fig. 1), which are used for (i) electrical resistivity measurement in the in-plane direction (specimen in the form of a beam of width about 2 mm and length about 25 mm, as measured separately for each specimen, obtained by making parallel cuts near a diameter of the disc, as indicated by B in Fig. 1), (ii) electrical resistivity measurement in the through-thickness direction (moon-shaped specimen, with largest width about 7 mm and largest length about 20 mm, as shown by D in Fig. 1), (iii) compressive testing (moon-shaped specimen, with largest width about 6 mm and largest length about 20 mm, as shown by E in Fig. 1), (iv) static flexural testing (specimen in the shape of a beam of width about 8 mm and length about 25 mm, as shown by C in Fig. 1) and (v) dynamic flexural testing (specimen in the shape of a beam of width about 8 mm and length about 30 mm, as shown by A in Fig. 1).

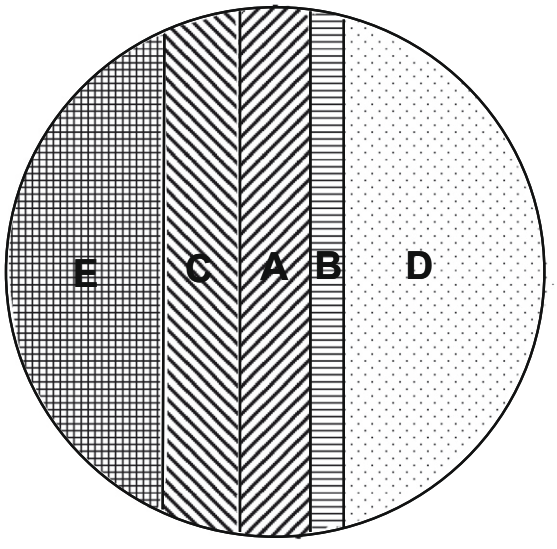

Fig. 1 – Geometry of specimens obtained by cutting a disc for use in various types of test. B: specimen for in-plane electrical resistivity measurement (length 25 mm; width 2 mm); D: specimen for through-thickness electrical resistivity measurement (length 20 mm; width 7 mm); E: specimen for compression testing (length 20 mm; width 6 mm); C: specimen for static flexural testing (length 25 mm; width 8 mm); A: specimen for dynamic flexural testing (length 30 mm; width 8 mm).

The proportion of exfoliated graphite to cement is controlled by weighing, so that the ratio of the volume of cement to the volume of graphite in the resulting composite (after compression but before curing) is 7:1, 9:1 or 12:1. With cement proportions exceeding that of 12:1, the graphite is not sufficient to bind the cement particles through mechanical interlocking of the exfoliated graphite during compression. Two discs are tested for each composition. The volume ratio is calculated from the measured weight ratio, with the density of the flexible graphite component of the composite taken as the measured density of the unmodified flexible graphite made in this work (0.82 g/cm^3, which is 0.36 of the value of 2.26 g/cm^3 for ideal graphite, i.e., 64% porosity) and the density of cement taken as 3.15 g/cm^3.

Dynamic flexural testing (ASTM D 4065-94) at a controlled frequency of 0.2 Hz is conducted at room temperature under three-point bending using a dynamic mechanical analyzer (DMA7, Perkin Elmer Corp., Norwalk, CT). The frequency of 0.2 Hz is chosen due to the relevance of low frequencies to large structures and the monotonic decrease of the loss tangent with increasing frequency from 0.2 Hz to 2.0 Hz [16]. The span is 20 mm. The loads used are large enough that the amplitude of the specimen deflection ranges from 5 to 10 μm (which is over the minimum value of 5 μm required by the equipment for accurate results). The storage modulus (elastic modulus under dynamic loading, i.e., the real part of the complex modulus) is measured at a static load range of 40 to 70 mN (static flexural stress of 0.25 MPa) and a dynamic load range of 30–60 (dynamic flexural stress of 0.2 MPa). Measurements of the loss tangent (tan δ) and storage modulus are made simultaneously. The damping ratio is half of the loss tangent (also called the loss factor). The loss modulus is the product of the loss tangent and the storage modulus.

The static flexural properties are measured under three-point bending (span = 20 mm) up to failure. A Sintech 2/D (MTS Systems Corp., Marblehead, MA) screw-action mechanical testing system is used. The flexural modulus is obtained from the slope of the resulting curve of flexural stress versus midspan deflection.

Compressive testing is conducted using a hydraulic mechanical testing system (MTS Model 810). The controlled displacement rate is 0.5 mm/min. For each specimen, testing is conducted up to failure. From the slope of the stress–strain curve near the origin, the compressive modulus is determined.

The electrical resistivity is measured by using the four-probe method, with silver paint in conjunction with copper wire or foil serving as electrical contacts. For measuring the in-plane resistivity, the electrical contacts are in the form of lines (of width about 1 mm) applied perimetrically around the specimen strip, such that the outer contacts (for passing current) are about 23 mm apart and the inner contacts (for voltage measurement) are about 15 mm apart. For measuring the through-thickness resistivity, (i) each of the two current contacts on the two opposite in-plane surfaces of a specimen is in the form of a copper foil with silver paint between the

foil and the specimen, such that the foil covers the entire in-plane surface of the specimen, except for a centered rectangular opening of edge length about 4 mm along the length of the moon shape and about 2 mm along the width of the moon shape, and (ii) each of the two voltage contacts is in the form of silver paint in conjunction with copper wire applied as a dot (diameter about 2 mm) within the rectangular opening mentioned above. A Keithley Model 224 programmable DC current source is used to provide a current, which is around 0.1 A, and is exactly measured by using a standard resistor (of resistance similar to that of the specimen, i.e., 0.1 Ω for in-plane resistance measurement and 0.001 Ω for through-thickness measurement) that is electrically in series with the specimen. A Keithley Model 2001 DC digital multimeter is used for measuring the voltage between the two voltage contacts of the specimen.

3. Results and discussion

Table 1 shows that the storage modulus, loss modulus, loss tangent and damping figure of merit all increase with increasing cement content in the cement–graphite composite. The increase in storage modulus is due to the high stiffness of cement compared to graphite. The increase in loss tangent is due to the increased degree of two-dimensionality (as indicated by the increased resistivity anisotropy (Table 3) and the consequent increase in the ease of shear of the graphite.

Flexure is a common mode of loading. Table 3 and Fig. 2(a) show that the flexural strength and modulus increase with increasing cement content. The flexural strength is higher than the value of 5.6 MPa for unmodified cement paste [29], whereas the flexural modulus is lower than the value of 5.9 GPa for unmodified cement paste [29].

Table 3 and Fig. 2(b) show that the compressive strength and modulus increase with increasing cement content. The compressive strength is much higher than the value of 58 MPa for unmodified cement paste [30], whereas the compressive modulus is much lower than the value of 2.9 GPa for unmodified cement paste [30]. The compressive strain at failure (ductility) decreases with increasing cement proportion. However, the strain is very high (0.38 or 38%, Fig. 2(b)) even for the highest cement proportion, compared to the value of 1.7% for unmodified cement paste [30]. The low values of the compressive and flexural moduli (Table 3) relate to the high strain.

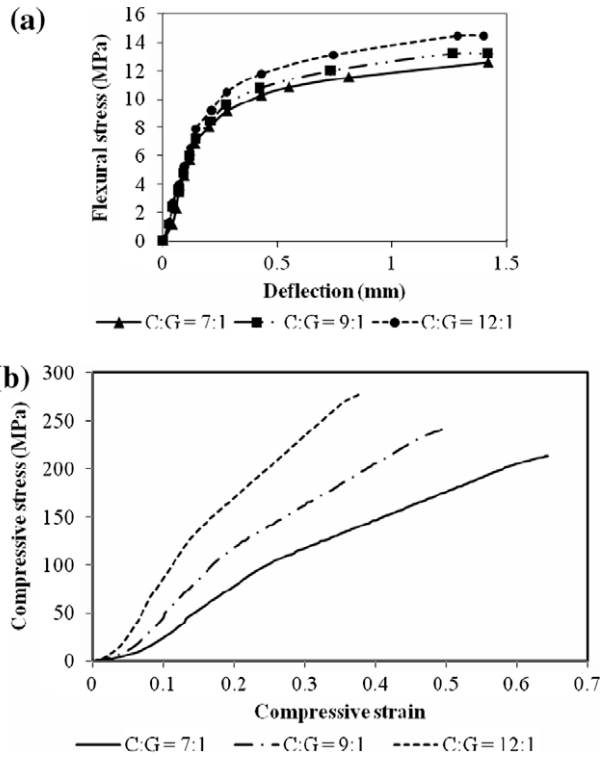

Fig. 2 – Static mechanical behavior of cement–graphite composites with three cement–graphite (C:G) ratios. (a) Flexural stress versus midspan deflection during static loading up to failure. (b) Compressive stress–strain curve static loading up to failure.

Table 3 shows that the in-plane and through-thickness resistivities and the through-thickness/in-plane resistivity ratio all increase with increasing cement content. For the same cement content, the through-thickness resistivity is much higher than the in-plane resistivity, indicating preferred in-plane orientation of the graphite basal plane. A higher value of the resistivity ratio means more two-dimensionality. Hence, the higher the cement proportion, the more is the two-dimensionality. The highest in-plane resistivity of 0.036 Ω cm and the highest through-thickness resistivity of 0.48 Ω cm, both obtained at the highest cement proportion, are considerably lower than the lowest value of 1 Ω cm previously reported for cement–matrix composites containing con-

Table 3 – Static mechanical properties, electrical resistivity and density of the cement–graphite composites of this work.

Cement/graphite ratio in mix	7:1	9:1	12:1
Graphite volume fraction[a]	0.13	0.10	0.077
Compressive strength (MPa)	213 ± 10	241 ± 8	278 ± 12
Compressive modulus (GPa)	0.332 ± 0.043	0.488 ± 0.045	0.729 ± 0.052
Flexural strength (MPa)	12.68 ± 0.84	13.24 ± 0.66	14.50 ± 1.10
Flexural modulus (GPa)	2.45 ± 0.25	2.82 ± 0.34	3.35 ± 0.35
Density (g/cm^3)	1.95	2.05	2.16
In-plane resistivity (10^{-3} Ω cm)	13 ± 7	20 ± 5	36 ± 9
Through-thickness resistivity (10^{-3} Ω cm)	100 ± 10	240 ± 10	480 ± 10
Through-thickness/in-plane resistivity ratio	8.3	12	13

a Before curing. The value is slightly lower after curing.

ductive admixtures, such as steel and carbon microfibers at volume fractions above the percolation threshold [31]. This means that the electrical connectivity of the graphite in the cement–graphite composites is superior to that of cement containing a conductive microfiber beyond the percolation threshold. This superiority is attributed to the mechanical interlocking of the exfoliated graphite. The interlocking makes the graphite a network, which is believed to help the damping ability of the composite. The network can undergo shear deformation, in contrast to the limited extent of shear deformation for a composite with a high-shear filler (such as rubber) that is discontinuous. For the unmodified cement paste, the resistivity is high, namely $10^5\ \Omega$ cm [32].

For flexible graphite without cement and prepared by similar compression of the same exfoliated graphite, the in-plane resistivity is 0.002 Ω cm, the through-thickness resistivity is 0.04 Ω cm and the through-thickness/in-plane resistivity ratio is 20. Hence, the resistivities and resistivity ratio of the cement–graphite composites are higher than those of flexible graphite. The higher resistivity ratio of flexible graphite means that flexible graphite is more two-dimensional than the cement–graphite composites.

Table 3 also shows the density of the composites. The density increases with decreasing graphite proportion. The values are comparable to that of 2.01 g/cm^3 for unmodified cement paste [30]. The rather high value of the density of

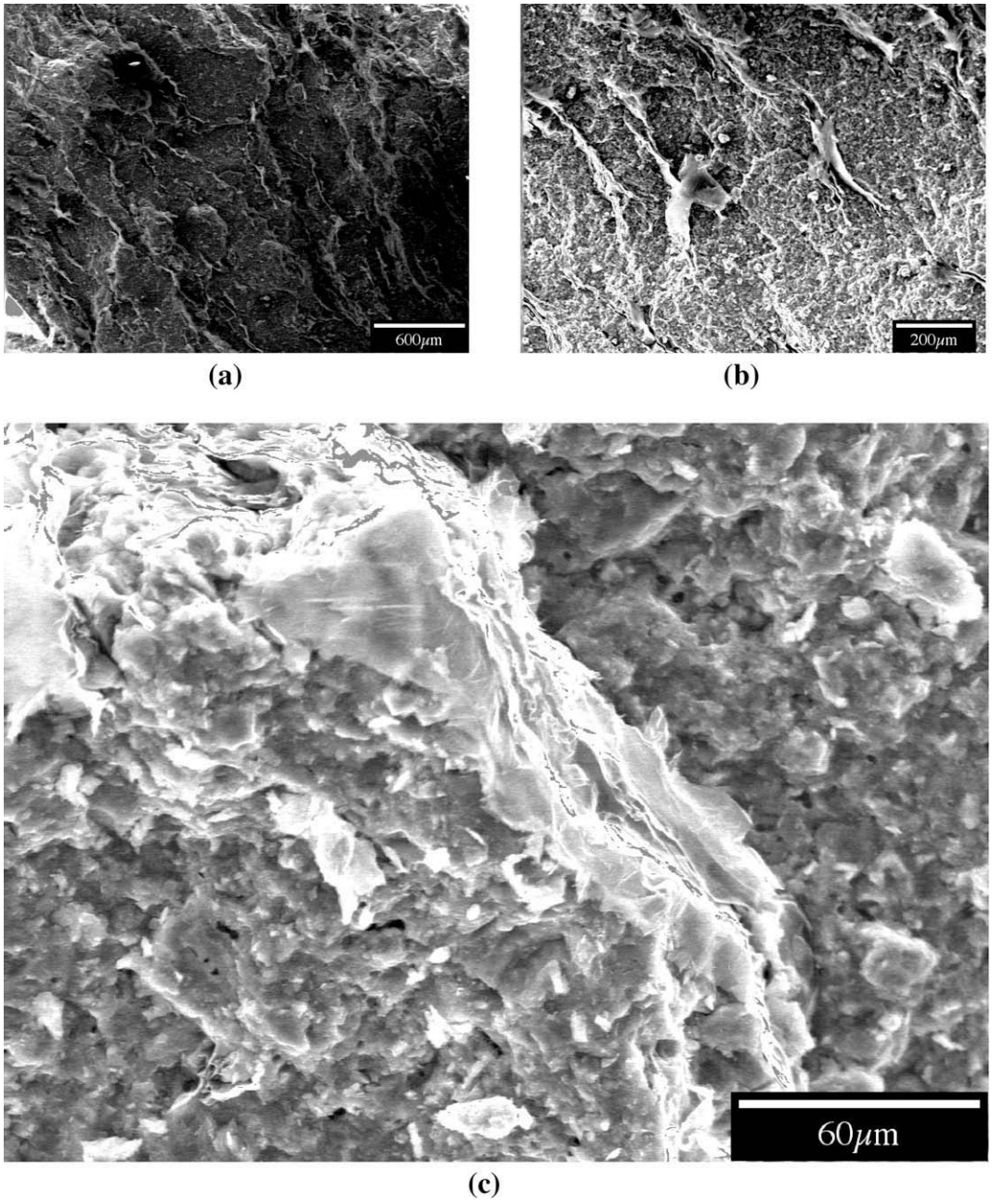

Fig. 3 – Scanning electron microscope photographs of the fracture surface of the composite with 12:1 cement:graphite ratio, as obtained after static flexural testing up to failure.

the composite with the highest cement proportion suggests that the porosity is low, as expected from the conformability (squishability) of the exfoliated graphite. The low porosity contributes to the high compressive strength and high flexural strength. Due to the low porosity, this composite is expected to be low in water permeability (not measured). A low permeability is valuable for the corrosion resistance of steel reinforced cement-based materials.

Fig. 3 shows scanning electron microscope (SEM) photographs of the fracture surface of the composite with cement–graphite proportion 12:1, as obtained after static flexural testing up to failure. The lowest magnification photograph (Fig. 3(a)) shows graphite as protruding ridges that are preferentially in the plane of the specimen. This preferred orientation is consistent with the electrical anisotropy. The ridges suggest the occurrence of shear in the graphite. In addition, Fig. 3(a) shows indications of a graphite network. The ridges are shown more clearly as bright regions in the intermediate magnification photograph (Fig. 3(b)). The highest magnification photograph (Fig. 3(c)) shows an intimate interface between graphite (bright region) and the cement matrix. This is consistent with the rather high density (Table 3). In addition, Fig. 3(c) shows the accordion microstructure within the graphite region. For the composites with lower cement proportions, SEM photographs show greater proportions of graphite.

The mechanical connectivity of the exfoliated graphite in the composite allows the graphite network as a whole to respond to vibrations. The ability of the network to respond to vibrations as a whole is in contrast to a less desirable situation in which parts of the network respond to vibrations individually. Physical connectivity (touching) without mechanical connectivity will not allow the graphite network as a whole to respond to vibrations. The ability of the network to respond to vibrations as a whole is important for achieving high damping. The proportion of graphite in the composite is preferably high enough for the graphite network to form.

The exfoliated graphite is distributed in the composite in a microscopic scale. In other words, the graphite network is microscopic in scale, with the ligaments in the network being narrow (in the micrometer scale). This fine distribution of the graphite is important for achieving high damping.

The proportion of cement in the composite is preferably high enough for the cement to form a continuous matrix in the composite. The continuity of the cement is important for attaining a high value of the elastic modulus (or the storage modulus).

The cement–graphite composite with cement–graphite proportion 12:1 is the most attractive composite of this work. Compared to rubber and other polymers [33,34], its advantages are very high loss modulus, high loss tangent, high strength, high modulus, low electrical resistivity and superior oxidation resistance. Compared to metals, its advantages are very high loss tangent, high loss modulus, high ductility and low density.

Compared to conventional cement-based materials, the advantages of the composite of this work are very high compressive ductility, very high compressive strength, high flexural strength, high flexural toughness (area under the flexural stress–deflection curve) and low electrical resistivity, and its disadvantages are very low compressive modulus and low flexural modulus.

The cement–graphite composite may be used for replacing polymers and metals for damping. It may also be used with conventional concrete. In one example, it is used as an aggregate in concrete for improving the damping; the composite aggregate is preferably added to the concrete mix when it is only slightly cured, so that strong cementitious bonding results between the aggregate and the cement matrix of the concrete. In contrast, rubber (as that from used tires) used as an aggregate in concrete suffers from poor bonding with the cement matrix. As a result, the rubber aggregate results in losses in strength and elastic modulus, though the toughness is increased [34–37]. In another example, the cement–graphite composite is sandwiched by and cementitiously bonded to concrete for improving the damping ability of the concrete.

4. Conclusion

This paper reports a material with unprecedented vibration damping ability, as shown by high values of both the loss tangent and the loss modulus under flexure at 0.2 Hz at room temperature. The loss modulus (7.5 GPa) exceeds that of any previously reported material, including the best metal-based material, which suffers from a low loss tangent. The loss tangent (0.81) is comparable to or exceeds that of any previously reported material, including rubber, which suffers from a low loss modulus.

The best material of this work is a cement–matrix graphite network composite containing 8 vol.% graphite (cement–graphite proportion 12:1). It is made by compressing a mixture of cement particles and exfoliated graphite, which binds by mechanical interlocking, followed by curing in water. The graphite network structure is supported by microscopy, which also shows an intimate interface between graphite and cement and an accordion microstructure within the graphite. The graphite network is also supported by the low electrical resistivity of the composite (0.04 Ω cm perpendicular to the compression direction and 0.5 Ω cm in the compression direction, indicating preferred in-plane orientation of the graphite basal plane). The composite is much more conductive than the most conductive previously reported cement–matrix composite containing a conductive admixture. The high loss tangent is attributed to the graphite network, while the high storage modulus is attributed to the cement matrix.

The material of this work exhibits high values of the compressive strength, flexural strength and compressive ductility compared to unmodified cement. However, its exhibits low values of the compressive and flexural moduli. The density is comparable to that of unmodified cement.

The loss tangent, loss modulus, storage modulus, damping figure of merit, in-plane and through-thickness resistivities, through-thickness/in-plane resistivity ratio, compressive strength and modulus, flexural strength and modulus, and density, all increase with increasing cement proportion. The compressive strain at failure (ductility) decreases with increasing cement proportion. The highest possible cement proportion corresponds to the lowest graphite proportion of

8 vol.% graphite. Beyond this cement proportion, there is inadequate graphite to hold the cement particles after compression (before cement curing).

REFERENCES

[1] Lu H, Wang X, Zhang T, Cheng Z, Fang Q. Design, fabrication, and properties of high damping metal matrix composites – a review. Materials 2009;2(3):958–77.

[2] Sharma SC, Krishna M, Shashishankar A, Vizhian SP. Damping behavior of aluminium/short glass fibre composites. Mater Sci Eng 2004;A364(1–2):109–16.

[3] Wang WG, Li C, Li YL, Wang XP, Fang QF. Damping properties of $Li_5La_3Ta_2O_{12}$ particulates reinforced aluminum matrix composites. Mater Sci Eng 2009;A518(1–2):190–3.

[4] San Juan J, No ML, Schuh CA. Nanoscale shape-memory alloys for ultrahigh mechanical damping. Nature Nanotechnol 2009;4(7):415–9.

[5] Schmidt I, Lammering R. The damping behavior of superelastic NiTi components. Mater Sci Eng 2004;A378(1–2):70–5.

[6] Corro ML, Kustov S, Cesari E, Chumlyakov YI. Magnetomechanical damping in Ni–Fe–Ga poly and single crystals. Mater Sci Eng A 2009;521–2:201–4.

[7] Lopez GA, Barrado M, San Juan J, No ML. Mechanical spectroscopy measurements on SMA high-damping composites. Mater Sci Eng 2009;A521–2:359–62.

[8] Shimazu T, Maeda H, Ishida EH, Miura M, Isu N, Ichikawa A, et al. High-damping and high-rigidity composites of Al_2TiO_5–$MgTi_2O_5$ ceramics and acrylic resin. J Mater Sci 2009;44:93–101.

[9] Andjelkovic DD, Lu Y, Kessler MR, Larock RC. Novel rubbers from the cationic copolymerization of soybean oils and dicyclopentadiene 2 – mechanical and damping properties. Marcromol Mater Eng 2009;294(8):472–83.

[10] Liu Q, Ding X, Zhang H, Yan X. Preparation of high-performance damping materials based on carboxylated nitrile rubbers combination of organic hybridization and fiber reinforcement. J Appl Polym Sci 2009;114(5):2655–61.

[11] Goyanes SN, Konig PG, Marconi JD. Dynamic mechanical analysis of particulate-filled epoxy resin. J Appl Polym Sci 2003;88:883–92.

[12] Senthilvelan S, Gnanamoorthy R. Damping characteristics of unreinforced, glass and carbon fiber reinforced nylon 6/6 spur gears. Polym Testing 2006;25:56–62.

[13] Babkina NV, Lipatov YS, Alekseeva TT. Damping properties of composites based on interpenetrating polymer networks formed in the presence of compatibilizing additives. Mech Compos Mater 2006;42(4):385–92.

[14] Jenkins MJ, Hine PJ, Hay JN, Ward IM. Mechanical and acoustic frequency responses in flat hot-compacted polyethylene and polypropylene panels. J Appl Polym Sci 2006;99:2789–96.

[15] Sarkhel G, Choudhury A. Dynamic mechanical and thermal properties of PE-EPDM based jute fiber composites. J Appl Polym Sci 2008;108:3442–53.

[16] Fu X, Chung DDL. Vibration damping admixtures for cement. Cement Concrete Res 1996;26(1):69–75.

[17] Xu Y, Chung DDL. Cement-based materials improved by surface treated admixtures. ACI Mater J 2000;97(3):333–42.

[18] Fu X, Li X, Chung DDL. Improving the vibration damping capacity of cement. J Mater Sci 1998;33:3601–5.

[19] Duan Z, Luo J. Effect of multi-walled carbon nanotubes on the vibration–reduction behavior of cement. In: Proceedings of the SPIE – the international society for optical engineering, vol. 6423, issue Pt. 1, international conference on smart materials and nanotechnology in engineering; 2007. p. 64230R/1–6.

[20] Fu W, Chung DDL. Vibration reduction ability of polymers, particularly polymethylmethacrylate and polytetrafluoroethylene. Polym Polym Compos 2001;9(6):423–6.

[21] Chung DDL. Materials for vibration damping. J Mater Sci 2001;36(24):5733–8.

[22] Wen S, Chung DDL. Thermoelectric behavior of carbon–cement composites. Carbon 2002;40:2495–505.

[23] Guerrero VH, Wang S, Wen S, Chung DDL. Thermoelectric property tailoring by composite engineering. J Mater Sci 2002;37(19):4127–36.

[24] Bhattacharya S, Sachdev VK, Chatterjee R, Tandon RP. Decisive properties of graphite-filled cement composites for device application. Appl Phys A 2008;92:417–20.

[25] Peinado F, Roig A, Vicente F. Electrochemical characterization of cement/graphite and cement/aluminium materials. J Mater Sci Lett 1994;13:609–12.

[26] Chung DDL. Exfoliation of graphite. J Mater Sci 1987;22(12):4190–8.

[27] Chung DDL. Flexible graphite for gasketing, adsorption, electromagnetic interference shielding, vibration damping, electrochemical applications, and stress sensing. J Mater Eng Perf 2000;9(2):161–3.

[28] Luo X, Chung DDL. Vibration damping using flexible graphite. Carbon 2000;38(10):1510–2.

[29] Segre N, Joekes I. Use of tire rubber particles as addition to cement paste. Cement Concrete Res 2000;30:1421–5.

[30] Chung DDL. Improving cement-based materials by using silica fume. J Mater Sci 2002;37(4):673–82.

[31] Wang S, Wen S, Chung DDL. Resistance heating using electrically conductive cements. Adv Cem Res 2004;16(4):161–6.

[32] Chung DDL. Electrically conductive cement-based materials. Adv Cem Res 2004;16(4):167–76.

[33] Datta RN, Huntink NM, Datta S, Talma AG. Rubber vulcanizates degradation and stabilization. Rubber Chem Technol 2007;80(3):436–80.

[34] Turatsinze A, Granju J-L, Bonnet S. Positive synergy between steel-fibres and rubber aggregates: effect on the resistance of cement-based mortars to shrinkage cracking. Cement Concrete Res 2006;36(9):1692–7.

[35] Khaloo AR, Dehestani M, Rahmatabadi P. Mechanical properties of concrete containing a high volume of tire-rubber particles. Waste Manage 2008;28:2472–82.

[36] Reda Taha MM, El-Dieb AS, Abd El-Wahab MA, Abdel-Hameed ME. Mechanical, fracture, and microstructural investigations of rubber concrete. J Mater Civil Eng 2008;20(10):640–9.

[37] Zheng L, Huo XS, Yuan Y. Strength, modulus of elasticity, and brittleness index of rubberized concrete. J Mater Civil Eng 2008;20(11):692–9.